

Co/Fe Selenides Hybrids: Hydrothermal Synthesis from Layered Double Hydroxides Precursor for Highly Efficient Oxygen Evolution Reaction

Jian Wan,^a Wen Ye,^b Rui Gao,^a Xiaoyu Fang,^b Zhenguo Guo,^a Yanluo Lu^{*a} and Dongpeng Yan^{*ab}

^a State Key Laboratory of Chemical Resource Engineering, Beijing University of Chemical Technology, Beijing 100029, (P. R. China).

^b Beijing Key Laboratory of Energy Conversion and Storage Materials, College of Chemistry, Beijing Normal University, Beijing 100875, P. R. China.

^c Jiangsu Key Laboratory of Advanced Catalytic Materials and Technology, Changzhou University, 213164, P. R. China.

*Correspondence address: D. Y. (E-mail: yandp@bnu.edu.cn); Y. L. (E-mail: luyl1@mail.buct.edu.cn).

Table of Contents

- 1 Experimental section
 - 1.1 Synthesis of Co₃Se₄&FeSe₂, Co₃Se₄, FeSe₂, RuO₂
 - 1.2 Characterizations
 - 1.3 Electrochemical measurements
- 2 Results and Discussion
- 3 Fig. S1 XRD patterns of CoFe selenide hybrids of different beginning ratio.
- 4 Fig. S2 SEM images of pristine Co₃Se₄.
- 5 Fig. S3 Polarization curves of CoFe selenide hybrids of different beginning ratio
- 6 Fig. S4 (a) Polarization curves of the Co₃Se₄, PM (Co₃Se₄ and FeSe₂ with physical mixing) and Co₃Se₄&FeSe₂. (b) Tafel plots of the Co₃Se₄, PM and Co₃Se₄&FeSe₂.
- 7 Fig. S5 (a) Polarization curves of the CoFe-LDH and Co₃Se₄&FeSe₂. (b) Tafel plots of the CoFe-LDH and Co₃Se₄&FeSe₂

- 8 Fig. S6 Faraday Efficiency of the OER catalyzed by $\text{Co}_3\text{Se}_4\&\text{FeSe}_2$ at 10 mA cm^{-2} in 1 M KOH solution
- 9 Fig. S7 Cyclic voltammetry curves of (a)the Co_3Se_4 . Cyclic voltammetry curves of (b)the PM. Cyclic voltammetry curves of (c)the $\text{Co}_3\text{Se}_4\&\text{FeSe}_2$. (d) The C_{dl} of the different samples obtained at $0.25 \text{ V vs. Ag/AgCl}$.
- 10 Fig. S8 Nyquist plots of Co_3Se_4 and $\text{Co}_3\text{Se}_4\&\text{FeSe}_2$.
- 11 Table S1 Comparison of OER performances between the $\text{Co}_3\text{Se}_4\&\text{FeSe}_2$ and recently reported materials.

1. Experimental section

Preparation of $\text{Co}_3\text{Se}_4\&\text{FeSe}_2$. The $\text{Co}_3\text{Se}_4\&\text{FeSe}_2$ hybrids were synthesized using $\text{Co}(\text{NO}_3)_2\cdot 6\text{H}_2\text{O}$, $\text{Fe}(\text{NO}_3)_3\cdot 9\text{H}_2\text{O}$, and Se powders as raw materials. 10 mmol of urea was first dispersed in a mixed solution consisting of 37 mL distilled water and 5 mL formamide. Then, $\text{Co}(\text{NO}_3)_2\cdot 6\text{H}_2\text{O}$ and $\text{Fe}(\text{NO}_3)_3\cdot 9\text{H}_2\text{O}$ were added into the dispersion under vigorous stirring. The molar ratio of Co/Fe varies from 1: 1 to 9: 1 (The total metal ion maintains 1 mmol and the corresponding products are marked as $\text{Co}_3\text{Se}_4\&\text{FeSe}_2(1-9)$, respectively. Next, 2 mmol Se powders and 3 mL $\text{N}_2\text{H}_4\cdot\text{H}_2\text{O}$ (80 wt%) were gradually added into the solution until the salt dissolved thoroughly. After sonication for one hour, the obtained mixture was transferred to an autoclave and heated at $180 \text{ }^\circ\text{C}$ for 16 h. Black solid can be obtained by centrifugation after the reaction system is heated and naturally cooled down to room temperature. To remove possible impurities such as excess salts that might exist, the solution was centrifuged for 5 times with deionized water and ethanol, respectively. After drying at $60 \text{ }^\circ\text{C}$ for 8 hours, the final product $\text{Co}_3\text{Se}_4\&\text{FeSe}_2$ can be obtained. It is noted that the $\text{Co}_3\text{Se}_4\&\text{FeSe}_2$ hybrid mentioned in this following section mainly refers to $\text{Co}_3\text{Se}_4\&\text{FeSe}_2(4)$.

Preparation of pristine Co_3Se_4 . Co_3Se_4 was synthesized using $\text{Co}(\text{NO}_3)_2\cdot 6\text{H}_2\text{O}$ and Se powders as raw materials. 10 mmol of urea was first dispersed in a mixed solution consisting of 37 mL distilled water and 5 mL formamide. Then, 1 mmol $\text{Co}(\text{NO}_3)_2\cdot 6\text{H}_2\text{O}$ was added into the dispersion under vigorous stirring. Next, 2 mmol Se powders and 3 mL $\text{N}_2\text{H}_4\cdot\text{H}_2\text{O}$ (80 wt%) were added gradually until the salt dissolved thoroughly. After sonication for one hour, the obtained mixture was transferred to an autoclave and heated at $180 \text{ }^\circ\text{C}$ for 16 h. Black solid was obtained by centrifugation after the reaction system is heated and naturally cooled

down to room temperature. The solution was centrifuged for 5 times with deionized water and ethanol, respectively. After drying at 60 °C for 8 hours, the final product Co_3Se_4 can be obtained.

Preparation of pristine FeSe_2 . FeSe_2 was synthesized using $\text{Fe}(\text{NO}_3)_3 \cdot 9\text{H}_2\text{O}$ and Se powders as raw materials. 10 mmol of urea was first dispersed in a mixed solution consisting of 37 mL distilled water and 5 mL formamide. Then, 1 mmol $\text{Fe}(\text{NO}_3)_3 \cdot 9\text{H}_2\text{O}$ were added into the dispersion under vigorous stirring. Next 2 mmol Se powders and 3 mL $\text{N}_2\text{H}_4 \cdot \text{H}_2\text{O}$ (80 wt%) were gradually added until the salt was dissolved thoroughly. After sonication for 1 hour, the obtained mixture was transferred to an autoclave and heated at 180 °C for 16 hours. Black solid was obtained by centrifugation after the reaction system is heated and naturally cooled to room temperature. The solution was centrifuged for 5 times with deionized water and ethanol, respectively. After drying at 60 °C for 8 hours, the final product FeSe_2 was obtained.

Preparation of RuO_2 . The preparation of RuO_2 is similar to the samples. 2 mg of RuO_2 and 50 μL of Nafion solution (5 wt %) were dispersed in the mixed solvent with 200 μL of ethanol and 750 μL of water under 1 hour sonication. And then the catalysts (5 μL) were drop-casted on the glassy carbon disk electrode at room temperature.

Characterization. The morphology, microstructure and chemical composition of the samples were characterized by field emission scanning electron microscopy (FESEM, Hitachi S-8010), transmission electron microscopy (TEM, JEOL, JEM-2100F), X-ray diffraction (XRD, Rigaku Ultima-IV), and X-ray photoelectron spectroscopy (XPS, Thermo VG ESCALAB MK II).

Electrochemical measurements. All tests were performed in a three-electrode system with CHI 660E electrochemical workstation. Glassy carbon disk electrode with diameters of 3 mm was prepared as working electrode, and Ag/AgCl electrode (with saturated KCl solution) and platinum wire were as reference and counter electrodes, respectively. In order to clean the working electrode, necessary pretreatment processes were performed. The working electrodes were polished with two different alpha alumina powders (1.0 and 0.3 μm) suspended in deionized water on a nylon polishing pad and with gamma alumina powder (0.05 μm) suspended in distilled water on a micro-cloth polishing pad. To obtain a homogeneous catalyst ink, 2 mg of sample and 50 μL of Nafion solution (5 wt %) were dispersed in the mixed solvent with 200 μL of ethanol and 750 μL of water under 1 hour

sonication. And then the catalysts (5 μL) were drop-casted on the glassy carbon disk electrode at room temperature. All electrochemical tests were conducted in 1 M KOH solution. All potentials were calibrated to a reversible hydrogen electrode (RHE). Passing half an hour of nitrogen to the potassium hydroxide solution prior to testing is necessary. In order to obtain the accurate catalytic effect of the catalyst, cyclic voltammetry (CV) test with a scan rate of 100 mV was first performed for 30 cycles to stabilize it at 1600 rpm before the linear sweep voltammetry (LSV) test, and then LSV was measured from 0.2 V to 0.8 V vs. saturated Ag/AgCl at a scan rate of 5 mV/s. The polarization curve obtained each time is IR corrected. CV tests at different scan rate (10, 20, 40, 80, 100 mV/s) were used to calculate double-layer capacitance (C_{dl}), which is usually used to evaluate the active area in an electrochemical catalytic process. The C_{dl} was half of the slope by plotting $\Delta j (j_a - j_c)$ against the scan rates, where j_a and j_c are the anodic and cathodic current densities, respectively. The electrochemical impedance spectrum (EIS) was also carried out with a frequency ranging from 0.1 Hz to 100 kHz at 450 mV vs. saturated Ag/AgCl and an AC amplitude of 5 mV. The long term stability test was taken with overpotential of 290mV.

The Faradaic efficiency was calculated by comparing the amount of gas theoretically calculated and experimentally measured. The Faradaic yield was calculated from the total amount of charge Q (C) passed through the cell and the total amount of oxygen produced (n_{O_2} : mmol). Assuming that four electrons are needed to produce one O_2 molecule, the Faradaic efficiency was calculated as faradaic efficiency $FE\% = n \times 4F/Q$, Where F is the Faraday constant, $Q = I \times t$ (C), and t is the time (s) for the constant oxidation current. The amount of oxygen produced in electrolysis was measured by a Neo-FOX oxygen-sensing system (Ocean Optics Inc.) with a FOXY-OR 125 probe inserted into the headspace of a gastight electrochemical cell. The electrochemical cell was filled with 1 M KOH. Then the oxygen probe was inserted into the headspace of a gastight electrochemical cell. The headspace was purged by nitrogen for one hour to establish a baseline in oxygen concentration (0%). A constant current density of 10 mA cm^{-2} was then passed for 120 min.

2. Results and discussion

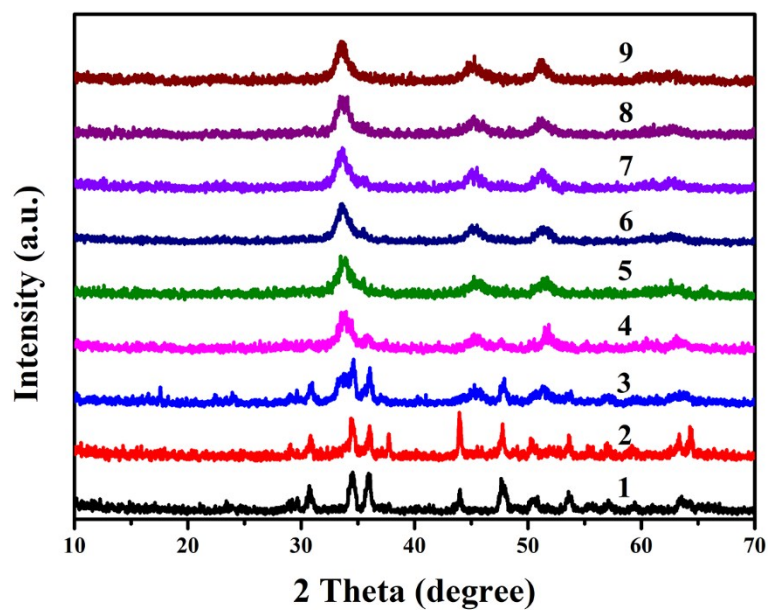


Fig. S1 XRD patterns of CoFe selenide hybrids of different beginning ratio (The numbers represent corresponding ratio between Co and Fe).

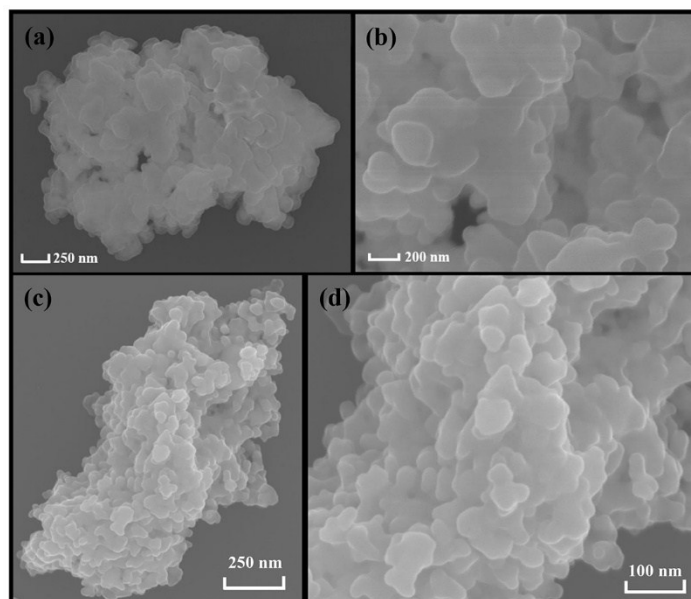


Fig. S2 (a), (b) SEM image of $\text{Co}_3\text{Se}_4/\text{FeSe}_2$, and (c), (d) SEM image of pristine Co_3Se_4

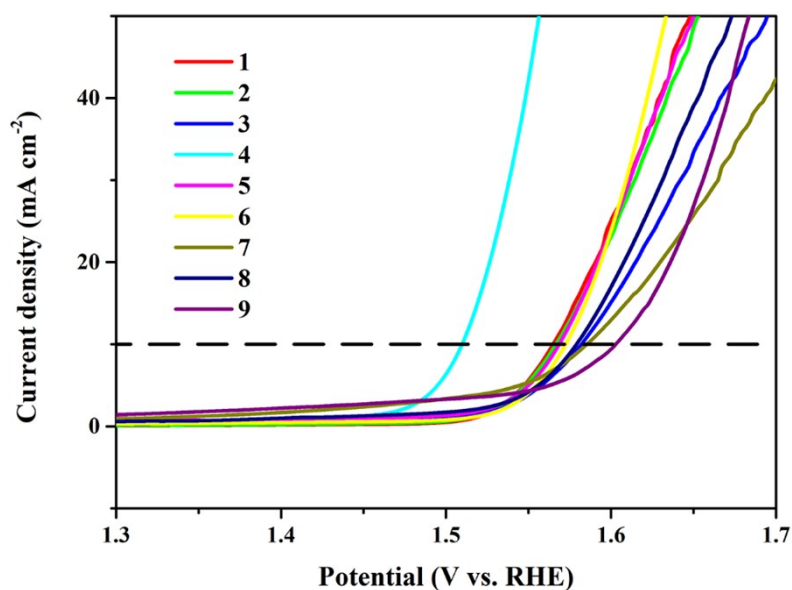


Fig. S3 Polarization curves of CoFe selenide hybrids of different beginning ratio (The numbers represents corresponding ratio between Co and Fe).

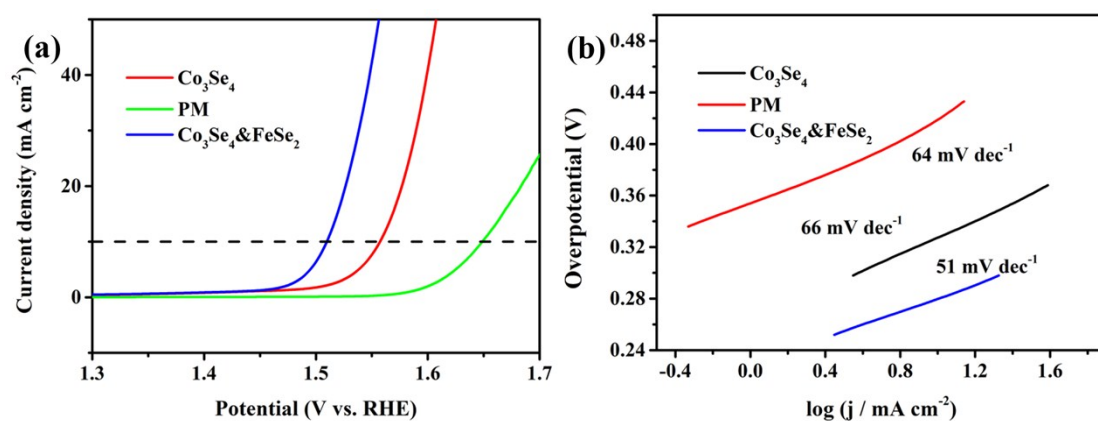


Fig. S4 (a) Polarization curves of the Co₃Se₄, PM (Co₃Se₄ and FeSe₂ with physical mixing) and Co₃Se₄&FeSe₂. (b) Tafel plots of the Co₃Se₄, PM and Co₃Se₄&FeSe₂.

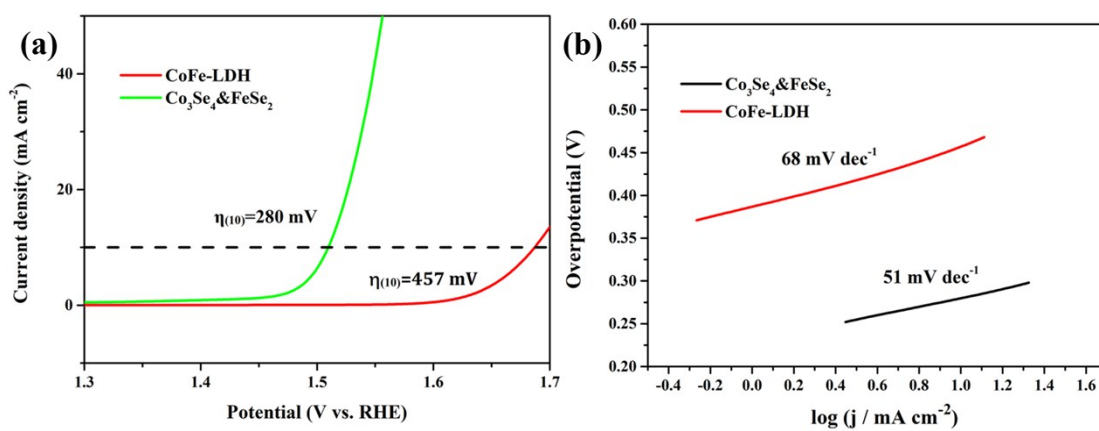


Fig. S5 (a) Polarization curves of the CoFe-LDH and Co₃Se₄&FeSe₂. (b) Tafel plots of the CoFe-LDH and Co₃Se₄&FeSe₂

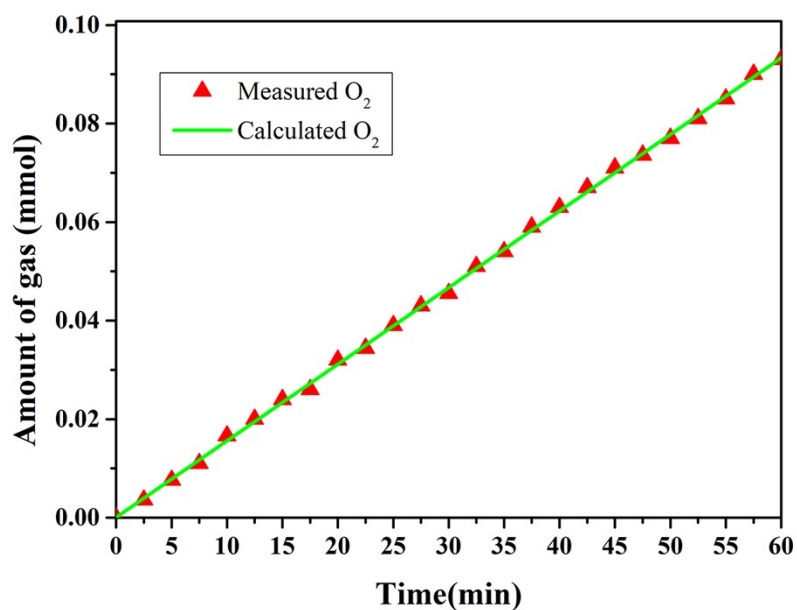


Fig. S6 Faraday Efficiency of the OER catalyzed by $\text{Co}_3\text{Se}_4\&\text{FeSe}_2$ at 10 mA cm^{-2} in 1 M KOH solution

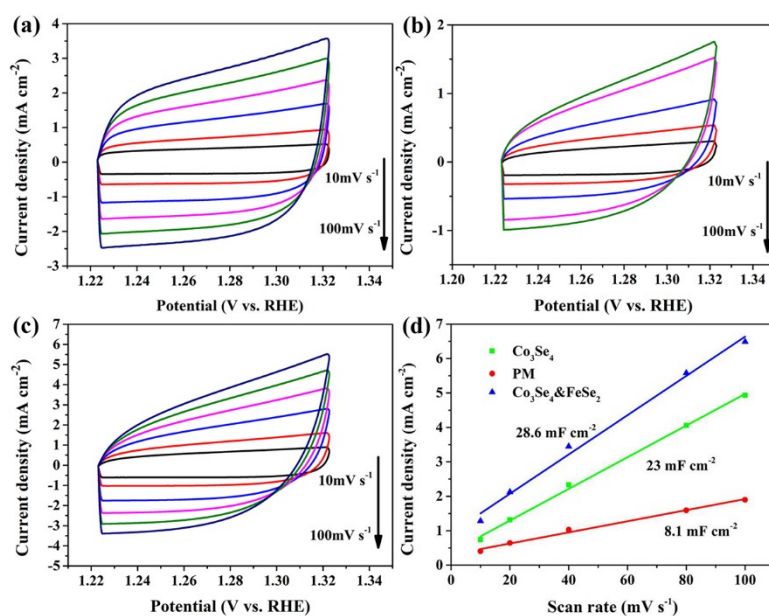


Fig. S7 Cyclic voltammetry curves of (a)the Co_3Se_4 . Cyclic voltammetry curves of (b)the PM. Cyclic voltammetry curves of (c)the $\text{Co}_3\text{Se}_4\&\text{FeSe}_2$. (d) The C_{dl} of the different samples obtained at 0.25 V vs. Ag/AgCl.

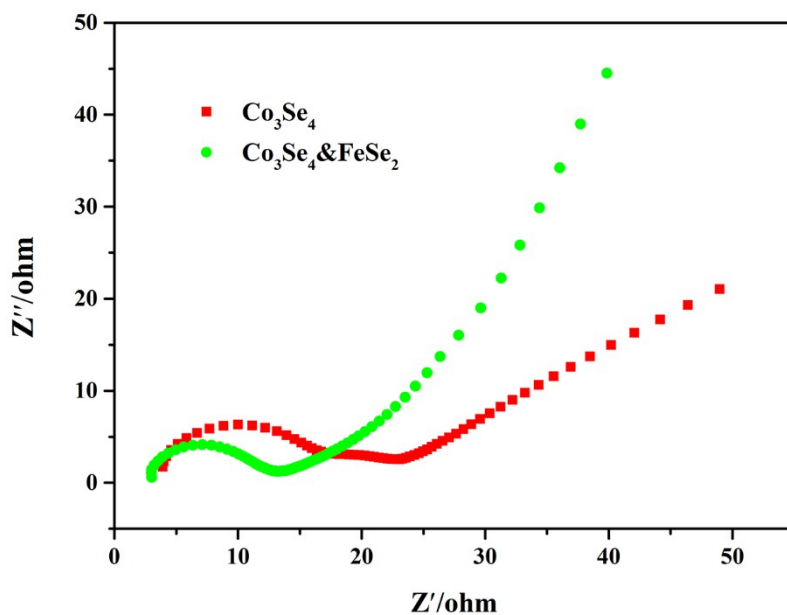


Fig. S8 Nyquist plots of Co_3Se_4 and $\text{Co}_3\text{Se}_4\&\text{FeSe}_2$.

Table S1 Comparison of OER performance between the $\text{Co}_3\text{Se}_4\&\text{FeSe}_2$ and recently reported materials.

Catalysts	Substrate	Overpotential (mV)	Tafel slope (mV dec^{-1})	References
$\text{Co}_3\text{Se}_4\&\text{FeSe}_2$	RDE	$\eta_{(10)} = 280$	51	this work
$\text{Co}_3\text{Se}_4/\text{CF}$	cobalt foam	$\eta_{(397)} = 320$	44	1
$\text{Co}_{0.85}\text{Se}/\text{CFC}$	Carbon fiber	$\eta_{(10)} = 324$	85	2
$\text{EG}/\text{Co}_{0.85}\text{Se}/\text{NiFe-LDH}$	exfoliated graphene	$\eta_{(150)} = 270$	57	3
$\text{Au}_{25}/\text{CoSe}_2$	GC	$\eta_{(10)} = 430$	—	4
CoSe_2	carbon cloth	$\eta_{(10)} = 290$	115	5
CoSe	Ti mesh	$\eta_{(10)} = 292$	69	6
CoSe_2	GC	$\eta_{(10)} = 430$	67	7
FeSe_2	nickel piece	$\eta_{(10)} = 330$	48	8
$\text{Co}_{0.75}\text{Fe}_{0.25}\text{-Se}$	nickel foam	$\eta_{(10)} = 246$	41	9

REFERENCES

- 1 W. Li, X. F. Gao, D. H. Xiong, F. Wei, W. G. Song, J. Y. Xu and L. F. Liu, *Adv. Energy Mater.*, 2017, **7**, 1602579.
- 2 C. Xia, Q. Jiang, C. Zhao, M. N. Hedhili and H. N. Alshareef, *Adv. Mater.*, 2016, **28**, 77-85.
- 3 Y. Hou, M. R. Lohe, J. Zhang, S. H. Liu, X. D. Zhuang and X. L. Feng, *Energy Environ. Sci.*, 2016, **9**, 478-483.
- 4 S. Zhao, R. X. Jin, H. Abroshan, C. J. Zeng, H. Zhang, S. D. House, E. Gottlieb, H. J. Kim, J. C. Yang and R. C. Jin, *J. Am. Chem. Soc.*, 2017, **139**, 1077-1080.

- 5 T. Chen, S. Z. Li, J. Wen, P. B. Gui and G. J. Fang, *ACS Appl. Mater. Interfaces*, 2017, **9**, 35927-35935.
- 6 T. T. Liu, Q. Liu, A. M. Asiri, Y. L. Luo and X. P. Sun, *Chem. Commun.*, 2015, **51**, 16683-16686.
- 7 I. H. Kwak, H. S. Im, D. M. Jang, Y. W. Kim, K. Park, Y. R. Lim, E. H. Cha J. Park, *ACS Appl. Mater. Interfaces*, 2016, **8**, 5327-5334.
- 8 R. Gao, H. Zhang and D. P. Yan, *Nano Energy*, 2017, **31**, 90-95.
- 9 K. L. Guo, Z. H. Zou, J. Du, Y. Q. Zhao, B. F. Zhou and C. Xu, *Chem. Commun.*, 2018, **54**, 11140-11143.